Distribution Agreement

In presenting this thesis or dissertation as a partial fulfillment of the requirements for an advanced degree from Emory University, I hereby grant to Emory University and its agents the non-exclusive license to archive, make accessible, and display my thesis or dissertation in whole or in part in all forms of media, now or hereafter known, including display on the world wide web. I understand that I may select some access restrictions as part of the online submission of this thesis or dissertation. I retain all ownership rights to the copyright of the thesis or dissertation. I also retain the right to use in future works (such as articles or books) all or part of this thesis or dissertation.

Signature:

_____ _____

Ziyin Tang Date

The Oxidative Potential of Fine Particulate Matter and Biological Perturbations in Human Plasma and Saliva Metabolome

By

Ziyin Tang
Master of Public Health

Environmental Health

_____

Donghai Liang, PhD, MPH
Committee Chair

The Oxidative Potential of Fine Particulate Matter and Biological Perturbations in Human Plasma and Saliva Metabolome

By

Ziyin Tang

B.M.
Southern Medical University
2019

Thesis Committee Chair: Donghai Liang, PhD, MPH

An abstract of
a thesis submitted to the Faculty of the
Rollins School of Public Health of Emory University
in partial fulfillment of the requirements for the degree of
Master of Public Health
in Environmental Health
2021

Abstract

The Oxidative Potential of Fine Particulate Matter and Biological Perturbations in Human Plasma and Saliva Metabolome

By Ziyin Tang

Background: Exposure assessment and health impact evaluation of particulate matter (PM) mixtures remain very challenging. Fine particle oxidative potential (FPMOP) has been considered as a key health-relevant particulate parameter. We measured FPMOP exposures in a recent panel study and corresponding metabolic perturbations to evaluate its potential epidemiologic value and examine molecular mechanisms underlying PM-related health impacts.

Methods: We recruited 54 participants from two dormitories in Atlanta, GA near and far from a congested highway. Indoor or outdoor FPMOP levels at the dormitories were measured using dithiothreitol (DTT) assay. Plasma and saliva samples were collected from participants at four time points during 12 weeks. Liquid chromatography coupled with high-resolution mass spectrometry was used to profile the participants' metabolome. We used mixed effect models to examine associations between metabolic features and FPMOP, controlling for potential confounders including age, gender, race, and body mass index. Significant metabolic features meeting false positive discovery rate at 20% were used for pathway enrichment analysis and metabolite annotation.

Results: The 96h-mean water soluble FPMOP levels at the near and far dormitories prior to biosample collection were 26.3 and 22.9 nmol/min/μg, respectively. In total, we extracted 20,766 metabolic features from plasma samples and 29,013 from saliva samples. Purine metabolism, N-glycan biosynthesis, and beta-alanine metabolism were most strongly associated with 5 or more FPMOP-related measurements in plasma, while vitamin E metabolism, leukotriene metabolism, and glycosphingolipid metabolism were found associated with FPMOP in saliva. We confirmed 6 metabolites directly associated with FPMOP measurements with level 1 evidence, including hypoxanthine, histidine, pyruvate, lactate/glyceraldehyde, azelaic acid, and petroselinic acid/elaidic acid/oleate, which were implications of perturbations in amino acid, carbohydrate, nucleotide and lipid metabolism.

Conclusions: We identified metabolites and pathways perturbations in plasma and saliva following by higher FPMOP exposure in panel-based setting. Perturbations in amino acid, carbohydrate, nucleotide and lipid metabolism may elicit PM-related health impacts.

The Oxidative Potential of Fine Particulate Matter and Biological Perturbations in Human Plasma and Saliva Metabolome

By

Ziyin Tang

B.M.
Southern Medical University
2019

Thesis Committee Chair: Donghai Liang, PhD, MPH

A thesis submitted to the Faculty of the
Rollins School of Public Health of Emory University
in partial fulfillment of the requirements for the degree of
Master of Public Health
in Environmental Health
2021

Acknowledgements

First and foremost, I am extremely grateful to my EH faculty and thesis advisor Dr. Donghai Liang for his patient guidance and continuous support throughout my master program. His rigorous attitude and passion to science has a profound influence on me. I would like to thank Dr. Jeremy Sarnat and the Environmental Metabolomics Group for their advices and help. I also want to express my gratitude to my family and friends. They gave me tremendous understanding and encouragement throughout my master program.

Table of Contents

Introduction.

Improving exposure assessment to particulate matter (PM) pollution is particularly critical given the abundance of epidemiological studies reporting associations between PM exposures and numerous adverse health effects (Feng et al. 2016; Mukherjee and Agrawal 2018). Toxicity of PM mixtures vary substantially by multiple aspects of particle properties, such as emission sources, species composition, size and surface properties (Lippmann and Chen 2009; Nel 2005). As a result, the exposure assessment and health impact evaluation of PM mixtures remain very challenging.

Recent interest in PM pollution health effects and regulatory intervention has shifted towards adopting multipollutant perspectives, where a multipollutant framework provides new opportunities to characterize external and internal exposures for highly heterogeneous PM mixtures. Specifically, oxidative potential of fine particulate matter (FPMOP), has emerged as a biologically-relevant, cumulative method for characterizing PM exposures through its ability to elicit reactive oxygen species (ROS). Previous studies have suggested a small mass-fraction of aerosol components, such as specific organic compounds (e.g., polycyclic aromatic hydrocarbons and quinones) and redox active metals, may drive most of the FPMOP, and hence toxicity (Charrier and Anastasio 2012; A. K. Cho et al. 2005). Generally, the formation of ROS by FPMOP is higher than the natural antioxidant capacity, and therefore, it may lead to a variety of PM-related adverse health outcomes (Delfino et al. 2011; Xia et al. 2006). Thus, FPMOP has been considered as a more biologically-relevant parameter to identify the adverse health effects of PM than mass concentration (Ayres et al. 2008; Bates et al. 2015; Borm et al. 2007). The dithiothreitol (DTT) assay is commonly used to measure FPMOP, which mimics interactions between cellular reductants and aerosol fractions in vivo through an acellular chemical analysis (Gao et al. 2017). An increasing number of studies found that $FPMOP^{DTT}$ was associated with several

cardiorespiratory endpoints, such as asthmas, lung cancers, and congestive heart failure (Bates et al. 2019). However, the underlying molecular mechanisms of FPMOP toxicity remain largely unclear, due to the lack of sensitive and specific biomarkers.

With the advancement in high-throughput analytical techniques, high-resolution metabolomics (HRM) offers great promise for detecting a very large number of exogenous toxicants and endogenous metabolites in microliter volumes of biosample, thereby providing improved capabilities for profiling complex heterogeneous toxicant exposures and associated metabolic perturbations in human samples (Bundy et al. 2008; Lankadurai et al. 2013). Using the untargeted Metabolome-Wide Association Study (MWAS) workflow, a hypothesis-driven method to analyze metabolome data without prior knowledge of identities, several studies, including those conducted by our group, have identified metabolic perturbations in proinflammatory and oxidative stress pathways on participants exposed to elevated $PM_{2.5}$ (Chen et al. 2019; Huang et al. 2018; Ladva et al. 2018; Li et al. 2017; Li et al. 2021; Liang et al. 2018b; Liang et al. 2019). While yielding important findings for future hypothesis generating studies, all of these existing projects use mass concentrations for PM exposure assessment, and none characterize the oxidative potential of PM mixtures. How PM oxidative potential contribute to molecular alternations in biological pathways and subsequent adverse health impacts still remain unknown.

To address these knowledge gaps, we conducted the present analysis to evaluate metabolic perturbation associated with FPMOP with the goal of identifying metabolomics-based measurements for FPMOP exposure and providing insights on the molecular mechanisms underlying PM-related health impacts.

Methods.

To evaluate the relationship between FPMOP indicators and corresponding metabolic perturbation in human body, we leveraged the FPMOP exposure data and high-resolution metabolomics profiling from the Dorm Room Inhalation to Vehicle Emission (DRIVE) study. The DRIVE study is an intensive 12-week field study that focused on comprehensively assessing exposures to primary traffic pollution along a full emission-to-exposure pathway. Detailed descriptions of DRIVE study have been previously described (Liang et al. 2018a; Moutinho et al. 2020a; Moutinho et al. 2020b; Sarnat 2018). Briefly, an intensive field sampling campaign took place between September 8, 2014 and January 5, 2015 on the campus of the Georgia Institute of Technology (GIT) in Atlanta, GA. GIT was adjacent to the Downtown Connector ("the Connector"), which was one of the most congested highway arteries in the United States (Figure 1). A suite of traffic- and non-traffic-related pollutants at 8 dedicated monitoring sites (6 outdoors and 2 indoors) were measured, and subsequently evaluated for their use as primary traffic exposure indicators in panel-based and small-cohort epidemiological studies. Concurrent with the field sampling, a panel of 54 non-smoking GIT students living in one of two dormitories located at different distances from the Connector were recruited for personal exposure measurement and repeated biomonitoring. Smoking was not permitted in buildings where both of two dormitories located. In addition, no predominant, known industrial emission points existed in the close proximity. The study protocol was approved and supervised by the Institutional Review Board at Emory University.

Exposure assessment on FPMOP. To characterize FPMOP indicators, we used two duplicate quartz filters to sample $PM_{2.5}$ every 48 hours during the study period at both the indoor and outdoor sites of two student dormitories for the DTT analyses, including the 'Near Dorm' (approximately

20 m west of the Connector) and the 'Far Dorm' (approximately 1.4 km west of the Connector) (Figure 1). To increase analytical sensitivity and accuracy in DTT quantitation, particle mass was extracted and composited from both of two duplicates filters for DTT analyses.

DTT acellular assay was used to characterize the oxidative potential of the water-soluble fraction of $PM_{2.5}$ (denoted as $FPMOP^{WS\text{-}DTT}$) based on its ability to catalyze electrons transfer from DTT to dissolved oxygen, resulting in DTT depletion and ROS generation. $FPMOP^{WS\text{-}DTT}$ normalized to $PM_{2.5}$ mass ($FPMOP^{WS\text{-}DTT}/\mu g$) was a measure of the intrinsic OP of the overall $PM_{2.5}$, which was an indication of the intrinsic OP in terms of $PM_{2.5.}$ $FPMOP^{WS\text{-}DTT}$ was normalized by volume of sampled air (expressed in units of pmol/min/m^3) to provide a measure of atmospheric concentration of aerosol OP (Sarnat 2018). $FPMOP^{total\text{-}DTT}$ considered both water-soluble and insoluble components of $PM_{2.5.}$ Briefly, in this measurement, water extracts from the air filter samples were not filtered (i.e. via liquid filtration) so that the insoluble particles could remain in the reaction aliquot and participate in the DTT consumption reaction (Sarnat 2018). This method has been validated and detailed previously (Gao et al. 2017).

Panel study participant recruitment. We recruited a panel of 54 students living in the Near Dorm and Far Dorm that housed the same indoor sampling instrumentation. Recruitment was conducted during a 3-week period to accommodate dorm move-in dates and the start of the fall school semester. Recruitment occurred on-site at the dorms by researchers in accordance to pre-established protocols and the Institutional Review Board at GIT. Of the 66 students who signed consent forms to participate in the study, 26 from the Near Dorm and 31 from the Far Dorm were enrolled based on an assessment of the subject's availability during the semester and likely compliance with the study protocol. During the 12-week personal sampling period, 2 subjects from the Near Dorm and 1 from the Far Dorm dropped out of the study. No specific reasons were given

for the attrition. In total, 54 students participated in the panel study and contributed to the biomonitoring.

High-resolution metabolomics profiling. High-resolution metabolome profiling was conducted on four (monthly) venous blood and twelve (weekly) saliva samples which were collected from each of 54 participants using established protocols (Go et al. 2015; Ladva et al. 2017; Li et al. 2021; Liang et al. 2018b). A total of 175 plasma samples and 621 2-ml vials of saliva were collected. Metabolome profiles on the monthly blood and saliva samples drew at the same time (September 19th, October 24th, November 14th and December 5th, 2014) were assembled for subsequent analyses. Liquid chromatography coupled with high-resolution mass spectrometry (LC-HRMS) techniques (Thermo Scientific^{TM} Q-Exactive^{TM} HF) were used to analyze biosamples, each of which was treated with two volumes of ice-cold acetonitrile prior to instrument analysis. To enhance the coverage of metabolic feature detection, two technical columns, the hydrophilic interaction liquid chromatography (HILIC) column with positive electrospray ionization (ESI) and C18 hydrophobic reversed-phase chromatography column with negative ESI, were utilized with triplicate runs of each sample. At the beginning and the end of each analytical batch of 20 samples, two quality control pooled human plasma samples including NIST 1950 (Simón-Manso et al. 2013) and pooled human plasma purchased from Equitech Bio were included for normalization, batch evaluation, background noise control, retention time alignment, and *post hoc* quantification. Raw metabolomics data files of all samples were then converted to .mzML files using ProteoWizard and extracted using apLCMS with modifications by xMSanalyzer(Uppal et al. 2013; Yu et al. 2009). Each detected signal (referred to as metabolic feature) was uniquely determined by the intensity of peak, mass-to-charge ratio (m/z) and retention time. Ultimately, to filter out noise signals and optimize the metabolomic data quality, only metabolic features detected in > 15% of

plasma/ saliva samples, exhibiting a median coefficient of variation (CV) among triplicate measures of < 30% as well as Pearson correlation > 0.7 were included in subsequent analyses. Triplicate measures were averaged followed by a $\log_2$ transformation.

Data analysis. We followed an established untargeted MWAS workflow, where we examined metabolomic changes associated with FPMOP-related indicators without prior metabolite validation. Given the longitudinal panel study design, linear mixed effect models were used to identify associations between intensity of metabolic features (i.e. relative concentration) and levels of different FPMOP-related indicators, adjusting for inter- and intra-individual variations. According to the logged GPS data, students had a relatively fixed time-activity pattern, with the majority of their time spent inside or around their respective dormitories (57% for students from near dormitory; 61% for students from far dormitory). Therefore, we selected $FPMOP^{DTT}$ measurements at these dormitories as a surrogate of actual personal exposures. 96h-average outdoor or indoor level of each of 5 FPMOP-related indicators ($FPMOP^{WS\text{-}DTT}$, $FPMOP^{WI\text{-}DTT}$, $FPMOP^{total\text{-}DTT}$, $FPMOP^{WS\text{-}DTT}/m^3$, $FPMOP^{WS\text{-}DTT}/\mu g$) at the dormitory locations were used as the primary exposures of interest. Separate models were conducted for each metabolic feature extracted from plasma and saliva using each of two analytical columns (plasma HILIC-positive column, plasma C18-negative column, saliva HILIC-positive column, and saliva C18-negative column). General forms of models were as follows:

$$log_2(Y_{ijt}) = \mu + \theta_i + \beta_{1j}FPMOP_{ikt} + \beta_{2j}\,Dormitory_i + \beta_{3j}Age_i + \beta_{4j}Gender_i + \beta_{5j}BMI_i + \beta_{6j}Race_i + \beta_{7j}Movingdays_{it} + \beta_{8j}\,Timepoints_{it} + \varepsilon_{ijkt} \quad (1)$$

where Y_{ijt} denotes intensity of metabolic feature j for participants i on date of sampling t. μ is the fixed-effect intercept and θ_i is the random effect included to control for potential inter-individual

variation. $FPMOP_{ikt}$ refers to the 96h-average outdoor or indoor level of FPMOP-related indicators k at the location of dormitory for participant i on biosampling date t. $Dormitory_i$ indicates the location of dormitory for participant i, which accounts for potential differences in the non-FPMOP-related factors among participants from two dormitories. To control for potential confounding, age (continuous), gender (categorical), body mass index (BMI; continuous), and race (categorical) were included as covariates. We also controlled for $Movingdays_{it}$ referring to the total number of days between the date t of biosamples collection and the date that participant i moved into the dormitory; and $Timepoint_{it}$ indicating the time point order of the biosamples collected from participant i on biosampling date t. ε_{ijkt} denotes residual random normal error.

Hypothesis tests to identify differentially expressed features associated with each of FPMOP-related indicators in each of biosamples from each of analytical columns were corrected for multiple comparisons using Benjamini-Hochberg false discovery rate ($FDR_{B\text{-}H}$) procedure at 20% false positive thresholds. The significant metabolic features ($FDR_{B\text{-}H} < 0.2$) associated with each of FPMOP-related indicators were used as input for pathway enrichment analysis and were further included in metabolite annotation process.

Pathway enrichment analysis and metabolite annotation. Each set of significant metabolic features with $FDR_{B\text{-}H} < 0.2$ associated with each of FPMOP-related indicators from each of four biomatrix columns will be separately used as input for pathway enrichment analysis using *mummichog* (v.1.0.9). *Mummichog* is a novel bioinformatics platform that infers and categorizes functional biological activity directly from mass spectrometry characteristics of metabolic features without confirmation of their identities (Li et al. 2013). An adjusted p-value for each pathway was

calculated from resampling the reference input file in *mummichog* using a gamma distribution. Pathways with fewer reference hits would be penalized, whereas pathways with more reference hits would be assigned greater significance (Li et al. 2013). Final results were presented in a metabolic-pathway-FPMOPs heat map, where each cell represented a statistical association between each of the significant pathways and each of the corresponding FPMOP-related indicators.

The metabolic features ($FDR_{B-H} < 0.2$) significantly associated with at least one FPMOP-related indicators were annotated by matching *m/z* value for adducts commonly formed to the Human Metabolome Database (HMDB), Kyoto Encyclopedia of Genes and Genomes (KEGG) (http://www.genome.jp/kegg/pathway.html), ChemSpider (http://www.chemspider.com/), and METLIN (https://metlin.scripps.edu) databases. Furthermore, the metabolic features ($FDR_{B-H} < 0.2$) significantly associated with at least one FPMOP-related indicators were annotated by matching accurate *m/z* value to authentic reference standards analyzed using the identical method and instrument parameters. A mass error threshold of 10 ppm was used in both of these two matching processes. For tentative matches, we further screened on the quality of peak by manual examination of extracted ion chromatograph (EIC) plots. Finally, these annotated metabolites will be confirmed with level one evidence by comparison of accurate mass m/z, retention time and ion dissociation patterns to analytical standards (Goodacre et al. 2007).

Results.

In the analysis, we included a total of 175 plasma samples (average of 3.2 repeated samples per participant) and 204 saliva samples (average of 3.8 repeated samples per participant) at four time points from 54 participants who provided blood and saliva samples. To reduce the exposure assessment error, we excluded the extreme outliers of FPMOP-related measurements beyond the

corresponding lower outer fence (the first quartile − 3* interquartile range) and upper outer fence (the third quartile + 3* interquartile range) from the analyses. Consequently, a total of 6 extreme outliers were removed. Mean indoor levels of $FPMOP^{WS\text{-}DTT}$, $FPMOP^{total\text{-}DTT}$ and $FPMOP^{WS\text{-}DTT}/m^3$ during the 12 weeks when the biomonitoring took place were significantly higher in the Far Dorm compared to those measured at the Near Dorm (Pooled *t*-Test: $p < 0.05$). Other indoor and outdoor levels of FPMOP-related indicators in two dormitories were not significantly different (Table 2, Figure 2). In terms of the information collected from each participant at baseline, demographic characteristics among participants in two dormitories were not significantly different (Table 1).

Continuous logged GPS data were collected from a subset of 43 participants over the study period of 12 sampling weeks, of which 21 from the Near Dorm and 22 from the Far Dorm. Clear bimodal distribution of time-activity patterns between participants from two dormitories were displayed, which indicated that students tended to spend majority of their time within or near their respective dormitories (Figure S1).

After instrument analysis followed by data quality filtering, we detected 20,766 metabolic features in plasma samples (HILIC-plasma column: 13,419; C18-plasma column: 7,347) and 29,013 in saliva samples (HILIC-saliva column: 21,313; C18- saliva column: 7,700). The median CV across triplicate measures of each metabolic feature was 24.8%, indicating good data quality (Liang et al. 2018b).

We conducted 40 sets of MWAS models (5 indoor/ outdoor FPMOP-related indicators among metabolic features in plasma and saliva, with each analyzed using two technical columns). In total, 967, 545, 1,214 and 412 unique metabolic features were associated with at least one or more of

the indoor or outdoor FPMOP-related indicators in HILIC-plasma, C18-plasma, HILIC-saliva, and C18-saliva columns, respectively ($FDR_{B\text{-}H} < 0.2$) (Table 3).

Pathway enrichment analysis indicated that 13 metabolic pathways were associated with at least 5 or more indoor or outdoor FPMOP-related indicators in plasma samples (Figure 3), while 19 significant metabolic pathways were detected in saliva samples (Figure 4). We observed 3 pathways consistently associated with various indoor or outdoor FPMOP-related indicators for both plasma and saliva samples analyzed using both technical columns, including leukotriene metabolism, galactose metabolism, and histidine metabolism. In plasma samples, purine metabolism, N-glycan biosynthesis and beta-alanine metabolism were most strongly associated with 5 or more the FPMOP-related measurements, while vitamin E metabolism, leukotriene metabolism and glycosphingolipid metabolism showed robust associations with FPMOPs in saliva samples. Significant perturbed pathways related to water soluble and insoluble FPMOP in both plasma and saliva were distinctly different. In plasma samples, purine metabolism and beta-alanine metabolism were most strongly associated with water soluble FPMOP, while aminosugars metabolism and purine metabolism were mostly strongly associated with water insoluble FPMOP (Figure 5). In saliva samples, the top two significant perturbed pathways associated with water soluble FPMOP were hexose phosphorylation and saturated fatty acids beta-oxidation, while bile acid biosynthesis and vitamin E metabolism were the top metabolic pathways associated with water insoluble FPMOP (Figure 6).

After matching these metabolic features with in-house analytical reference validated, we confirmed 6 metabolites with level 1 evidence, of which 1, 1, and 5 were from HILIC-plasma, HILIC-saliva C18-plasma (Table 4). Histidine was identified in both HILIC-saliva and C18-plasma columns. Except the positive association found between hypoxanthine and FPMOP, we

observed negative associations ($\beta < 0$) between these confirmed metabolites and corresponding associated FPMOP-related indicators. These confirmed metabolites were indicative of perturbations in amino acid metabolism (n=4, 36%), carbohydrate metabolism (n=5, 45%), nucleotide metabolism (n=1, 9%) and lipid metabolism (n=1, 9%).

Discussion.

Using the high-resolution metabolomics in combination with pathway enrichment analysis and chemical confirmation, we assessed the metabolic perturbations and potential pathways associated with a novel multipollutant measurement on PM mixtures– FPMOP. To our knowledge, this would be the first study to examine metabolic perturbation associated with $PM_{2.5}$ oxidative potential. By using FPMOP measurements, we identified several metabolites and perturbed pathways which have been associated with PM mass or PM components in earlier studies. We also observed distinctly different perturbed pathways significantly associated with water soluble and insoluble FPMOP, respectively in both plasma and saliva, suggesting that different pathways might mediate health impacts of water soluble and insoluble FPMOP. Ultimately, we confirmed identities of 6 metabolites, four of which were indicative of acute inflammation, nucleic acid damage and repair, and energy perturbation. The disturbance of these processes induced the generation of ROS that ultimately led to enhanced oxidative stress and inflammation (Figure 7).

During the 12 weeks when the biomonitoring occurred, exposure assessment results indicated that mean indoor levels of $FPMOP^{WS\text{-}DTT}$, $FPMOP^{total\text{-}DTT}$ and $FPMOP^{WS\text{-}DTT}/m^3$ were significantly higher in the Far Dorm compared to those measured at the Near Dorm (Pooled *t*-Test: $p < 0.05$), while other indoor and outdoor levels of FPMOP-related indicators at two dormitories were not significantly different. Our group reported earlier that outdoor levels of $PM_{2.5}$ were significantly

higher in the Near Dorm compared to Far Dorm (Liang et al. 2018b). Unlike outdoor $PM_{2.5}$ levels, outdoor FPMOP measurements were fairly spatially uniform. It suggested that atmospheric secondary processing further enhanced FPMOP, likely associated with the oxidation of primary polycyclic aromatic hydrocarbons to quinones and hydroxyquinones, and with the oxidization and water solubility of metals (Sarnat 2018).

In plasma samples, purine metabolism, N-glycan biosynthesis, and beta-alanine metabolism were most strongly associated with 5 or more FPMOP-related measurements. The perturbation of purine metabolism might lead to nucleic acid damage and repair, since purine metabolism has been closed linked with the formation and degradation of nucleic acid. Hypoxanthine, xanthine, and uric acid are three key components of purine metabolism. The processes of catalyzing the conversion of hypoxanthine to xanthine, and from the xanthine to uric acid generate superoxide anion and other reactive oxygen products, resulting in enhanced oxidative stress (Glantzounis et al. 2005). Uric acid was found to be an antioxidant and it accounts for half of the total antioxidant capacity of biological fluids in human (Glantzounis et al. 2005; Ndrepepa 2018). Several studies also identified perturbation of purine metabolism following exposure to higher level of $PM_{2.5}$ and several $PM_{2.5}$ species including ultrafine particles, black carbon, and some transitional metals (Mu et al. 2019; Nassan et al. 2021b). Consistently in this analysis, we confirmed hypoxanthine in plasma samples, which was found to be positively associated with exposure to indoor $FPMOP^{WS\text{-}DTT}$/μg. Two recent studies have also reported that the level of hypoxanthine increased in urine and serum samples as exposure level of $PM_{2.5}$ increased (Chen et al. 2019; Mu et al. 2019). However, two other studies have observed negative association between hypoxanthine and $PM_{2.5}$ exposure among asthmatic commuters and white men (Liang et al. 2019; Nassan et al. 2021a). The

discrepancy of the results may result from the variations in biomonitoring specimens, study populations, and exposure assessment methods.

We found N-glycans biosynthesis was significantly disturbed following exposures to FPMOP. N-glycans are glycoproteins consist of glycans and glycan chains linked to nitrogen atoms of amino acid residues, which have diverse functions and regulate multiple molecular behaviors (Chacko et al. 2011; Reily et al. 2019). N-glycans involves in immunity, inflammation, and development of several diseases such as Alzheimer's disease (Kizuka et al. 2017; Reily et al. 2019). Endothelial surface N-glycans can regulate the adhesion molecules that control the interactions between endothelial cells and leukocytes, which is the key in the development of vascular inflammatory disease (Chacko et al. 2011). Therefore, the perturbation of N-glycan biosynthesis may be indicative of damages in immunity and inflammatory response and then subsequent relevant diseases.

Beta-alanine metabolism was one of the pathways strongly perturbed by FPMOP-related indicators in plasma. Beta-alanine, a non-essential β-amino acid, occurs naturally in human central nervous system, which can act as either a neurotransmitter or a neuromodulator (Sale et al. 2010). The accumulation of beta-alanine level affects several important functions including delay in brain development, oxidative stress, and disturbances in energy metabolism (Gemelli et al. 2018). Several studies have associated beta-alanine metabolism perturbation with $PM_{2.5}$ and ultrafine particles (Jeong et al. 2018; Walker et al. 2019).

In saliva, vitamin E metabolism, leukotriene metabolism, and glycosphingolipid metabolism were found most strongly associated with 5 or more FPMOP-related measurements, and our findings were consistent with previous studies. Specifically, in our previous traffic-related air pollution-

MWAS analysis in the same panel, vitamin E metabolism and leukotriene metabolism were identified as the most significant perturbed pathways associated with majority of traffic-related air pollutants including black carbon (BC), carbon monoxide (CO), nitric oxide (NO), nitrogen dioxide (NO_2) , nitric oxides (NOx) and $PM_{2.5}$ in plasma (Liang et al. 2018b). In another independent panel of asthmatic and healthy commuter, these two pathways were again found to be significantly associated with exposure to $PM_{2.5}$, BC, organic carbon, elemental carbon, several transitional metals (Liang et al. 2019). Another study found leukotriene metabolism were significantly associated with ultrafine particles (Walker et al. 2019). These two pathways played important roles in xenobiotic-mediated oxidative stress and acute inflammatory response (Ching Kuang 1991; Henderson 1994; Singh et al. 2005). Meanwhile, glycosphingolipids metabolism has also been linked with $PM_{2.5}$, ultrafine particles and other $PM_{2.5}$ species exposure previously (Jeong et al. 2018; Liang et al. 2018b; Nassan et al. 2021a; Nassan et al. 2021b; Walker et al. 2019).

Earlier studies identified that DTT-active water-soluble fractions of PM include Humic-like substances (predominantly represents the hydrophobic organic fraction of $PM_{2.5}$), water soluble organic carbon, oxygenated quinones, and transition metals (Arthur K. Cho et al. 2005; Fang et al. 2016; Lin and Yu 2011; Verma et al. 2012). DDT-active water-insoluble species were found to be correlated with Humic-like substances, water-insoluble organic carbon and elemental carbon (Verma et al. 2012). Several cell and animal studies have reported the different toxic effects on neonatal rat cardiomyocytes and metabolic impacts in mice exerted by water soluble and insoluble $PM_{2.5}$ (Qi et al. 2019; Zhang et al. 2018). Interestingly, we observed distinctly different perturbed pathways significantly associated with more than two water soluble and insoluble FPMOP, respectively in both plasma and saliva. In plasma, there were only 3 common pathways including purine metabolism, histidine metabolism, and N-glycan biosynthesis potentially affected by both

water soluble and insoluble FPMOP using both HILIC and C18 chromatography columns. $FPMOP^{WS\text{-}DTT}$ exposure mainly influenced nucleotide metabolism (n=2, 20%), amino acid metabolism (n=2, 20%) and carbohydrate metabolism (n=2, 20%). $FPMOP^{WI\text{-}DTT}$ mainly perturbed amino acid metabolism (n=5, 33%), glycan biosynthesis and metabolism (n=4, 27%), and carbohydrate metabolism (n=3, 20%). In saliva, only one pathway was perturbed by both water soluble and insoluble FPMOP using both two technical columns. 9 out of 13 significant perturbed pathways associated with $FPMOP^{WI\text{-}DTT}$ identified in saliva using both technical columns belonged to lipid metabolism. Differences in significant perturbed pathways indicated that water soluble and insoluble OP may have different biological function and health impacts. Cautions shall be taken when interpreting these results, as the toxicity of water soluble and insoluble fraction of $PM_{2.5}$ was reflected by the ability of generating ROS, which didn't take account for their actual component characteristics. Further studies on exploration of specific metabolic perturbations of different chemical components of $PM_{2.5}$ are warranted to validate the current findings.

We also confirmed the identity of histidine, which was inversely associated with exposure to outdoor $FPMOP^{WS\text{-}DTT}$/μg. Histidine is an essential amino acid, involving in synthesizing histamine, a well-known mediator involved in inflammatory and regulatory functions on different body sites depending on the cell type and the receptor (Branco et al. 2018). Pathway results indicated that histidine lies in two significant perturbed pathways including histidine and beta-alanine metabolism. Consistently, decreased histidine was found to be associated with increased exposure to $PM_{2.5}$ in our previous MWAS study (Liang et al. 2018b). In addition, pyruvate and lactate were confirmed in present analysis. The perturbation of these two metabolites implied energy perturbation might mediate PM-related health impacts. Two animal studies showed that

exposure to $PM_{2.5}$ led to elevated levels of pyruvate and lactate in mice, suggesting that transformation of energy metabolism from the TCA cycle to glycolysis (Ning et al. 2019; Ran et al. 2021). In Mu et al., 2019, a positive association has been identified between lactate and short-term exposure to $PM_{2.5}$ (Mu et al. 2019). On the contrary, pyruvate and lactate were negatively associated with several indoor FPMOP-related indicators in our study. Consistently, lactate has been negatively associated with higher exposure level of $PM_{2.5}$ in other studies including our previous MWAS analysis (Liang et al. 2018b; Nassan et al. 2021a). Pyruvate was identified to be in several significant pathways including pyruvate metabolism, aminosugars metabolism, glycolysis and gluconeogenesis, purine metabolism, glycine, serine, alanine and threonine metabolism, tyrosine metabolism, whereas lactate lies in pyruvate metabolism and glycolysis and gluconeogenesis.

Despite these promising findings, the current analysis has several limitations. First, the relatively small sample size of this panel warrants attention, since the findings may be unduly influenced by individual participants. However, we conducted repeated biomonitoring over four time points for each participant, which could reduce intra-individual variations to some extents. Secondly, in the present analysis, we used FPMOP measurements at dormitories as surrogates of individual exposures, which may introduce measurement errors given the subjects did not stay at their dormitory locations all the time. In addition, 21.9% of FPMOP measurements from 48h quartz filter-based samples which were used to integrate the 96h average exposure levels were missing. In present analysis, only non-missing values were averaged and then used as exposure levels. In summary, the range of FPMOP exposure levels among participants were narrowed, which may obscure true associations between FPMOP and certain metabolic features. However, we were still able to identify hundreds of unique metabolic features significantly associated with the FPMOP.

Thirdly, there was a possibility of false positive discovery due to multiple testing in big data analysis. To minimize the risk of false positive discovery, we conducted a suite of quality assurance and control measures throughout the analysis. We decided to use less stringent criteria -- metabolic features at FDR < 20% in MWAS for subsequent analyses, which might increase the risk of false positives but would minimize the chance of false negatives. Additionally, changes in metabolome reflect the combined effects of endogenous and exogenous factors, which makes it difficult to characterize the metabolomic perturbation induced by single exposure. In our study, the repeated biomonitoring reduced intra-individual variations and the multiple confounders and covariates included in MWAS models may minimize the potential influences of factors other than FPMOP. Last but not least, with a limited number of authentic standard references from the in-house validation database, we were only able to confirm the identity of 6 metabolites with level 1 evidence out of hundreds of significant metabolic features in MWAS analysis, where we will likely miss potential important metabolic signals.

Conclusions.

In summary, by using FPMOP measurements, we identified several metabolites and perturbed pathways significantly associated with $PM_{2.5}$ oxidative potential. We observed different metabolic pathways associated with water soluble and insoluble FPMOP, respectively. Intriguingly, the significant perturbed pathways related to FPMOP measurements have been mostly linked to other air pollutants, suggesting that the air pollution may pose effects on human health through the disruption of similar biological processes other than specific pathways. The confirmed metabolites in present analysis mainly involved in acute inflammation, nucleic acid damage and repair, and energy perturbation. The disturbance of these processes may induce the generation of ROS that ultimately led to enhanced oxidative stress and systemic inflammation. These metabolites could

be further developed as sensitive biomarkers which reflects internal exposures to $PM_{2.5}$, and health responses related to oxidative stress and inflammation exerted by $PM_{2.5}$. Future hypothesis testing studies are warranted to validate these findings on specific metabolic perturbations of different chemical components of $PM_{2.5}$.

References.

Ayres JG, Borm P, Cassee FR, Castranova V, Donaldson K, Ghio A, et al. 2008. Evaluating the toxicity of airborne particulate matter and nanoparticles by measuring oxidative stress potential—a workshop report and consensus statement. Inhalation Toxicology 20:75-99.

Bates JT, Weber RJ, Abrams J, Verma V, Fang T, Klein M, et al. 2015. Reactive oxygen species generation linked to sources of atmospheric particulate matter and cardiorespiratory effects. Environ Sci Technol 49:13605-13612.

Bates JT, Fang T, Verma V, Zeng L, Weber RJ, Tolbert PE, et al. 2019. Review of acellular assays of ambient particulate matter oxidative potential: Methods and relationships with composition, sources, and health effects. Environ Sci Technol 53:4003-4019.

Borm PJA, Kelly F, Künzli N, Schins RPF, Donaldson K. 2007. Oxidant generation by particulate matter: From biologically effective dose to a promising, novel metric. Occupational and environmental medicine 64:73-74.

Branco ACCC, Yoshikawa FSY, Pietrobon AJ, Sato MN. 2018. Role of histamine in modulating the immune response and inflammation. Mediators Inflamm 2018:9524075-9524075.

Bundy JG, Davey MP, Viant MR. 2008. Environmental metabolomics: A critical review and future perspectives. Metabolomics 5:3-21.

Chacko BK, Scott DW, Chandler RT, Patel RP. 2011. Endothelial surface n-glycans mediate monocyte adhesion and are targets for anti-inflammatory effects of peroxisome proliferator-activated receptor γ ligands. J Biol Chem 286:38738-38747.

Charrier JG, Anastasio C. 2012. On dithiothreitol (dtt) as a measure of oxidative potential for ambient particles: Evidence for the importance of soluble transition metals. Atmos Chem Phys 12:11317-11350.

Chen C, Li H, Niu Y, Liu C, Lin Z, Cai J, et al. 2019. Impact of short-term exposure to fine particulate matter air pollution on urinary metabolome: A randomized, double-blind, crossover trial. Environ Int 130:104878.

Ching Kuang C. 1991. Vitamin e and oxidative stress. Free Radical Biology and Medicine 11:215-232.

Cho AK, Sioutas C, Miguel AH, Kumagai Y, Schmitz DA, Singh M, et al. 2005. Redox activity of airborne particulate matter at different sites in the los angeles basin. Environmental Research 99:40-47.

Cho AK, Sioutas C, Miguel AH, Kumagai Y, Schmitz DA, Singh M, et al. 2005. Redox activity of airborne particulate matter at different sites in the los angeles basin. Environ Res 99:40-47.

Delfino RJ, Staimer N, Vaziri ND. 2011. Air pollution and circulating biomarkers of oxidative stress. Air Qual Atmos Health 4:37-52.

Fang T, Verma V, Bates JT, Abrams J, Klein M, Strickland MJ, et al. 2016. Oxidative potential of ambient water-soluble pm_{2.5} in the southeastern united states: Contrasts in sources and health associations between ascorbic acid (aa) and dithiothreitol (dtt) assays. Atmospheric Chemistry & Physics 16:3865-3879.

Feng S, Gao D, Liao F, Zhou F, Wang X. 2016. The health effects of ambient pm2.5 and potential mechanisms. Ecotoxicology and Environmental Safety 128:67-74.

Gao D, Fang T, Verma V, Zeng L, Weber RJ. 2017. A method for measuring total aerosol oxidative potential (op) with the dithiothreitol (dtt) assay and comparisons between an urban and roadside site of water-soluble and total op. Atmospheric Measurement Techniques 10:2821-2835.

Gemelli T, de Andrade RB, Rojas DB, Zanatta Â, Schirmbeck GH, Funchal C, et al. 2018. Chronic exposure to β-alanine generates oxidative stress and alters energy metabolism in cerebral cortex and cerebellum of wistar rats. Molecular Neurobiology 55:5101-5110.

Glantzounis GK, Tsimoyiannis EC, Kappas AM, Galaris DA. 2005. Uric acid and oxidative stress. Curr Pharm Des 11:4145-4151.

Go YM, Walker DI, Liang Y, Uppal K, Soltow QA, Tran V, et al. 2015. Reference standardization for mass spectrometry and high-resolution metabolomics applications to exposome research. Toxicol Sci 148:531-543.

Goodacre R, Broadhurst D, Smilde AK, Kristal BS, Baker JD, Beger R, et al. 2007. Proposed minimum reporting standards for data analysis in metabolomics. Metabolomics 3:231-241.

Henderson WR, Jr. 1994. The role of leukotrienes in inflammation. Ann Intern Med 121:684-697.

Huang Q, Hu D, Wang X, Chen Y, Wu Y, Pan L, et al. 2018. The modification of indoor pm2.5 exposure to chronic obstructive pulmonary disease in chinese elderly people: A meet-in-metabolite analysis. Environ Int 121:1243-1252.

Jeong A, Fiorito G, Keski-Rahkonen P, Imboden M, Kiss A, Robinot N, et al. 2018. Perturbation of metabolic pathways mediates the association of air pollutants with asthma and cardiovascular diseases. Environ Int 119:334-345.

Kizuka Y, Kitazume S, Taniguchi N. 2017. N-glycan and alzheimer's disease. Biochimica et Biophysica Acta (BBA) - General Subjects 1861:2447-2454.

Ladva CN, Golan R, Greenwald R, Yu T, Sarnat SE, Flanders WD, et al. 2017. Metabolomic profiles of plasma, exhaled breath condensate, and saliva are correlated with potential for air toxics detection. J Breath Res 12:016008.

Ladva CN, Golan R, Liang D, Greenwald R, Walker DI, Uppal K, et al. 2018. Particulate metal exposures induce plasma metabolome changes in a commuter panel study. PLoS One 13:e0203468.

Lankadurai BP, Nagato EG, Simpson MJ. 2013. Environmental metabolomics: An emerging approach to study organism responses to environmental stressors. Environmental Reviews 21:180-205.

Li H, Cai J, Chen R, Zhao Z, Ying Z, Wang L, et al. 2017. Particulate matter exposure and stress hormone levels: A randomized, double-blind, crossover trial of air purification. Circulation 136:618-627.

Li S, Park Y, Duraisingham S, Strobel FH, Khan N, Soltow QA, et al. 2013. Predicting network activity from high throughput metabolomics. PLOS Computational Biology 9:e1003123.

Li Z, Liang D, Ye D, Chang HH, Ziegler TR, Jones DP, et al. 2021. Application of high-resolution metabolomics to identify biological pathways perturbed by traffic-related air pollution. Environ Res 193:110506.

Liang D, Golan R, Moutinho JL, Chang HH, Greenwald R, Sarnat SE, et al. 2018a. Errors associated with the use of roadside monitoring in the estimation of acute traffic pollutant-related health effects. Environ Res 165:210-219.

Liang D, Moutinho JL, Golan R, Yu T, Ladva CN, Niedzwiecki M, et al. 2018b. Use of high-resolution metabolomics for the identification of metabolic signals associated with traffic-related air pollution. Environ Int 120:145-154.

Liang D, Ladva CN, Golan R, Yu T, Walker DI, Sarnat SE, et al. 2019. Perturbations of the arginine metabolome following exposures to traffic-related air pollution in a panel of commuters with and without asthma. Environ Int 127:503-513.

Lin P, Yu JZ. 2011. Generation of reactive oxygen species mediated by humic-like substances in atmospheric aerosols. Environmental Science & Technology 45:10362-10368.

Lippmann M, Chen L-C. 2009. Health effects of concentrated ambient air particulate matter (caps) and its components. Critical Reviews in Toxicology 39:865-913.

Moutinho JL, Liang D, Golan R, Ebelt ST, Weber R, Sarnat JA, et al. 2020a. Evaluating a multipollutant metric for use in characterizing traffic-related air pollution exposures within near-road environments. Environ Res 184:109389.

Moutinho JL, Liang D, Golan R, Sarnat SE, Weber R, Sarnat JA, et al. 2020b. Near-road vehicle emissions air quality monitoring for exposure modeling. Atmos Environ (1994) 224.

Mu L, Niu Z, Blair RH, Yu H, Browne RW, Bonner MR, et al. 2019. Metabolomics profiling before, during, and after the beijing olympics: A panel study of within-individual differences during periods of high and low air pollution. Environ Health Perspect 127:57010.

Mukherjee A, Agrawal M. 2018. A global perspective of fine particulate matter pollution and its health effects. Rev Environ Contam Toxicol 244:5-51.

Nassan FL, Kelly RS, Kosheleva A, Koutrakis P, Vokonas PS, Lasky-Su JA, et al. 2021a. Metabolomic signatures of the long-term exposure to air pollution and temperature. Environ Health 20:3.

Nassan FL, Wang C, Kelly RS, Lasky-Su JA, Vokonas PS, Koutrakis P, et al. 2021b. Ambient pm2.5 species and ultrafine particle exposure and their differential metabolomic signatures. Environ Int 151:106447.

Ndrepepa G. 2018. Uric acid and cardiovascular disease. Clin Chim Acta 484:150-163.

Nel A. 2005. Atmosphere. Air pollution-related illness: Effects of particles. Science 308:804-806.

Ning X, Ji X, Li G, Sang N. 2019. Ambient pm2.5 causes lung injuries and coupled energy metabolic disorder. Ecotoxicology and Environmental Safety 170:620-626.

Qi Z, Song Y, Ding Q, Liao X, Li R, Liu G, et al. 2019. Water soluble and insoluble components of pm(2.5) and their functional cardiotoxicities on neonatal rat cardiomyocytes in vitro. Ecotoxicol Environ Saf 168:378-387.

Ran Z, An Y, Zhou J, Yang J, Zhang Y, Yang J, et al. 2021. Subchronic exposure to concentrated ambient pm2.5 perturbs gut and lung microbiota as well as metabolic profiles in mice. Environmental Pollution 272:115987.

Reily C, Stewart TJ, Renfrow MB, Novak J. 2019. Glycosylation in health and disease. Nat Rev Nephrol 15:346-366.

Sale C, Saunders B, Harris RC. 2010. Effect of beta-alanine supplementation on muscle carnosine concentrations and exercise performance. Amino Acids 39:321-333.

Sarnat JA, Russell, A. G., Liang, D., Moutinho, J. L., Golan, R., Weber, R. J., Gao, D., Sarnat, S. E., Chang, H. H., Greenwald, R., Yu, T. 2018. Developing multipollutant exposure indicators of traffic pollution: The dorm room inhalation to vehicle emissions (drive) study. 196.Health Effect Institute.

Simón-Manso Y, Lowenthal MS, Kilpatrick LE, Sampson ML, Telu KH, Rudnick PA, et al. 2013. Metabolite profiling of a nist standard reference material for human plasma (srm 1950): Gc-ms, lc-ms, nmr, and clinical laboratory analyses, libraries, and web-based resources. Analytical Chemistry 85:11725-11731.

Singh U, Devaraj S, Jialal I. 2005. Vitamin e, oxidative stress, and inflammation. Annual Review of Nutrition 25:151-174.

Uppal K, Soltow QA, Strobel FH, Pittard WS, Gernert KM, Yu T, et al. 2013. Xmsanalyzer: Automated pipeline for improved feature detection and downstream analysis of large-scale, non-targeted metabolomics data. BMC Bioinformatics 14:15.

Verma V, Rico-Martinez R, Kotra N, King L, Liu J, Snell TW, et al. 2012. Contribution of water-soluble and insoluble components and their hydrophobic/hydrophilic subfractions to the reactive oxygen species-generating potential of fine ambient aerosols. Environmental Science & Technology 46:11384-11392.

Walker DI, Lane KJ, Liu K, Uppal K, Patton AP, Durant JL, et al. 2019. Metabolomic assessment of exposure to near-highway ultrafine particles. J Expo Sci Environ Epidemiol 29:469-483.

Xia T, Kovochich M, Nel A. 2006. The role of reactive oxygen species and oxidative stress in mediating particulate matter injury. Clin Occup Environ Med 5:817-836.

Yu T, Park Y, Johnson JM, Jones DP. 2009. Aplcms--adaptive processing of high-resolution lc/ms data. Bioinformatics 25:1930-1936.

Zhang Y, Li Y, Shi Z, Wu J, Yang X, Feng L, et al. 2018. Metabolic impact induced by total, water soluble and insoluble components of pm(2.5) acute exposure in mice. Chemosphere 207:337-346.

Tables and Figures.

Figure 1. DRIVE study location. Yellow line represents the I-75/ I-85 interstate highway. Near Dorm is 20 m away from the highway and Far Dorm is 1400 m away from the highway.

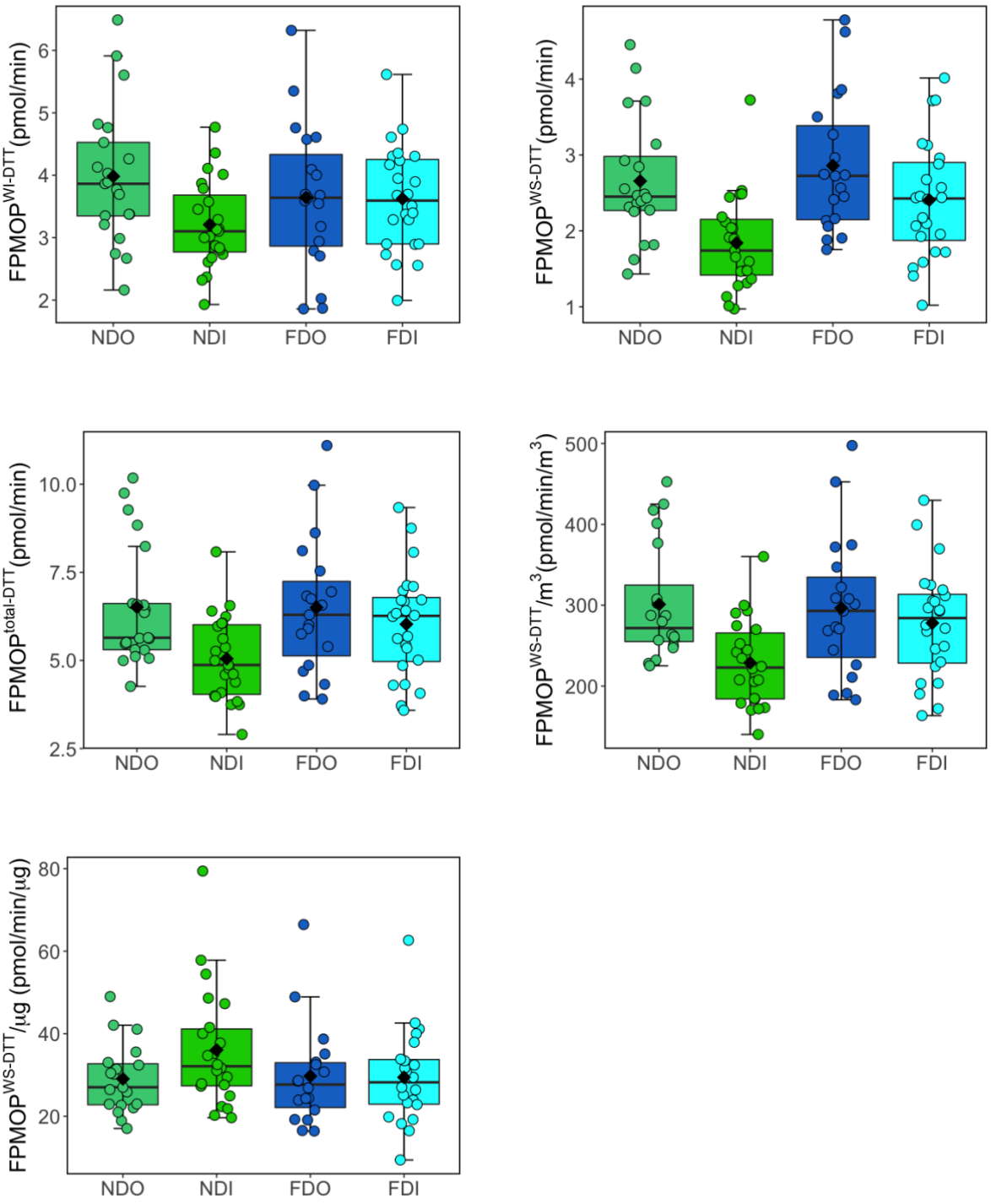

Figure 2. Boxplots presenting the distribution of $FPMOP^{WI\text{-}DTT}$, $FPMOP^{WS\text{-}DTT}$, $FPMOP^{total\text{-}DTT}$, $FPMOP^{WS\text{-}DTT}/m^3$, $FPMOP^{WS\text{-}DTT}/\mu g$ during September 8th, 2014 to December 15th, 2014 from 48-hour integrated filter measurements at dormitories.

Acronym: $FPMOP^{WI\text{-}DTT}$, oxidative potential of water-insoluble fraction in fine particulate matter; $FPMOP^{WS\text{-}DTT}$, oxidative potential of water-soluble fraction in fine particulate matter; $FPMOP^{total\text{-}DTT}$, oxidative potential of water-soluble fraction and water-insoluble fraction in fine particulate matter; $FPMOP^{WS\text{-}DTT}/m^3$, oxidative potential of water-soluble fraction in fine particulate matter normalized by the total volume of sampled air; $FPMOP^{WS\text{-}DTT}/\mu g$, oxidative potential of water-soluble fraction in fine particulate matter divided by overall fine particulate mass; NDO, outdoor side at Near Dorm; NDI, indoor side at Near Dorm; FDO, outdoor side at Far Dorm; indoor site at Far Dorm.

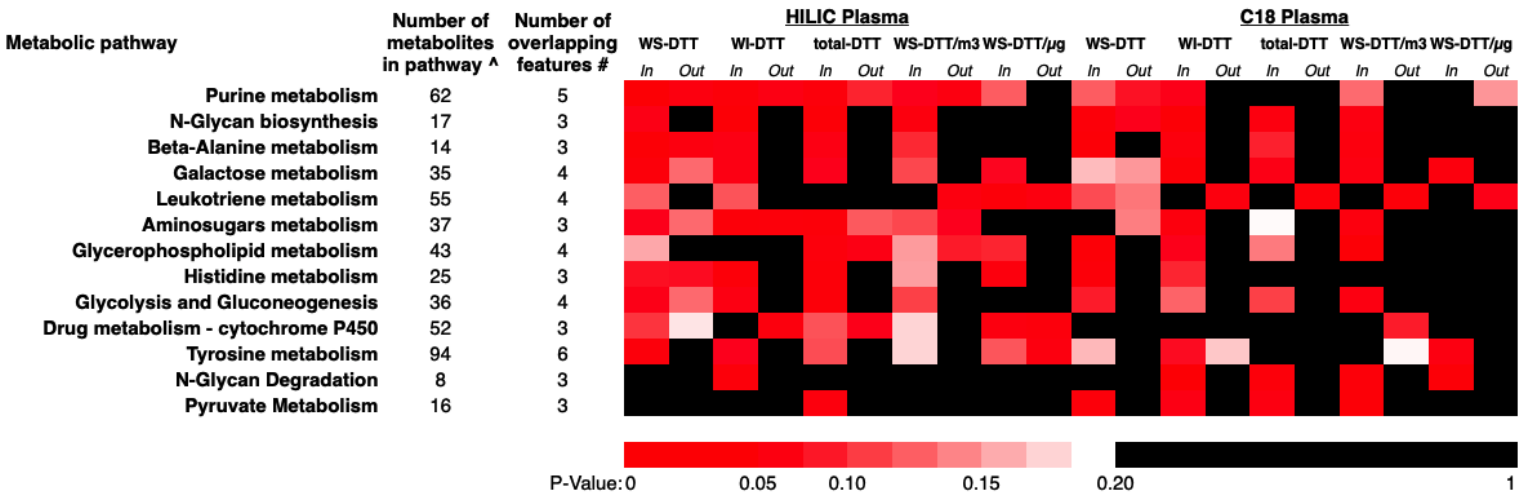

Figure 3. Metabolic pathways associated with ≥ 5 FPMOP-related indicators in plasma.
Cells were shaded based on the p-value of the association between each of metabolic pathways and each indoor/ outdoor FPMOP-related indicator. Metabolic pathways are ordered according to the total number of the significant pathway-FPMOP associations ($p < 0.05$) in the HILIC column and the C18 column.
^ Total number of metabolites within the specific metabolic pathway;
# Number of significant metabolic features in the biosamples with m/z matched to the metabolites within the specific metabolic pathway.

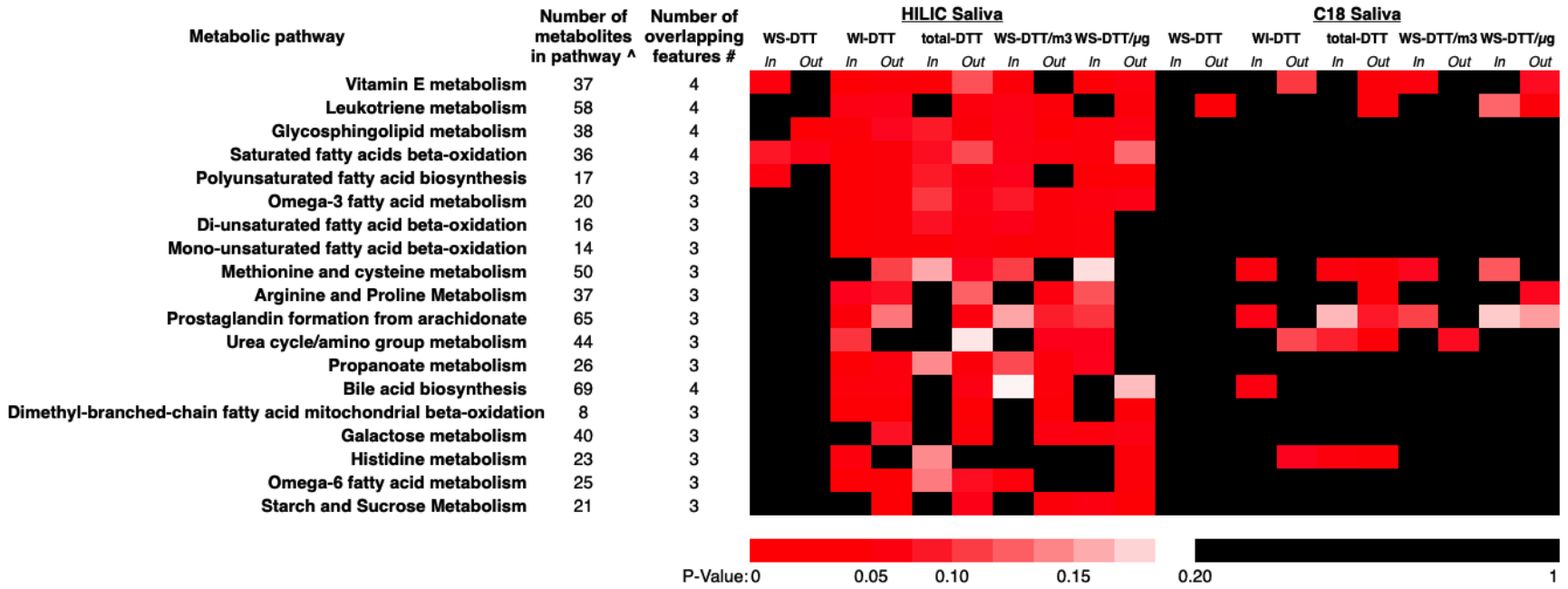

Figure 4. Metabolic pathways associated with ≥ 5 FPMOP-related indicators in saliva.
Cells were shaded based on the p-value of the association between each of metabolic pathways and each indoor/ outdoor FPMOP-related indicator. Metabolic pathways are ordered according to the total number of the significant pathway-FPMOP associations ($p < 0.05$) in the HILIC column and the C18 column.
^ Total number of metabolites within the specific metabolic pathway;
# Number of significant metabolic features in the biosamples with m/z matched to the metabolites within the specific metabolic pathway.

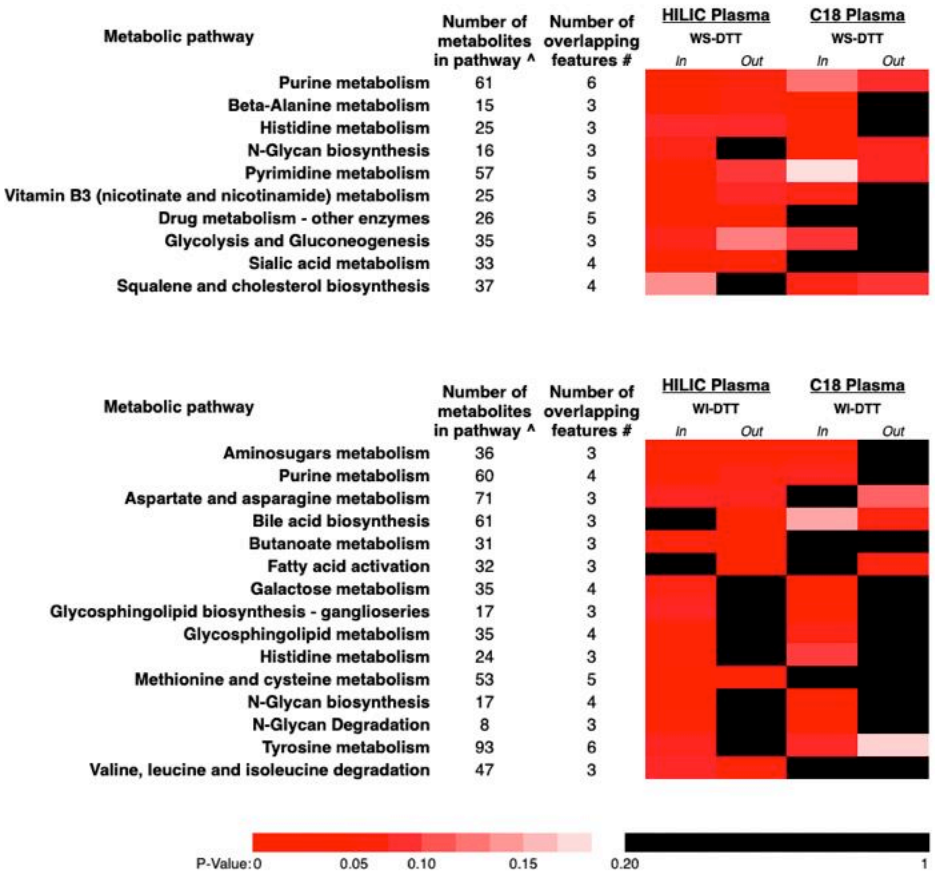

Figure 5. Metabolic pathways associated with ≥ 2 water soluable and insoluable FPMOP respectively in plasma.
Cells were shaded based on the p-value of the association between each of metabolic pathways and each indoor/ outdoor water soluble and insoluble FPMOP. Metabolic pathways are ordered according to the total number of the significant pathway-FPMOP associations ($p < 0.05$) in the HILIC column and the C18 column.
^ Total number of metabolites within the specific metabolic pathway;
# Number of significant metabolic features in the biosamples with m/z matched to the metabolites within the specific metabolic pathway.

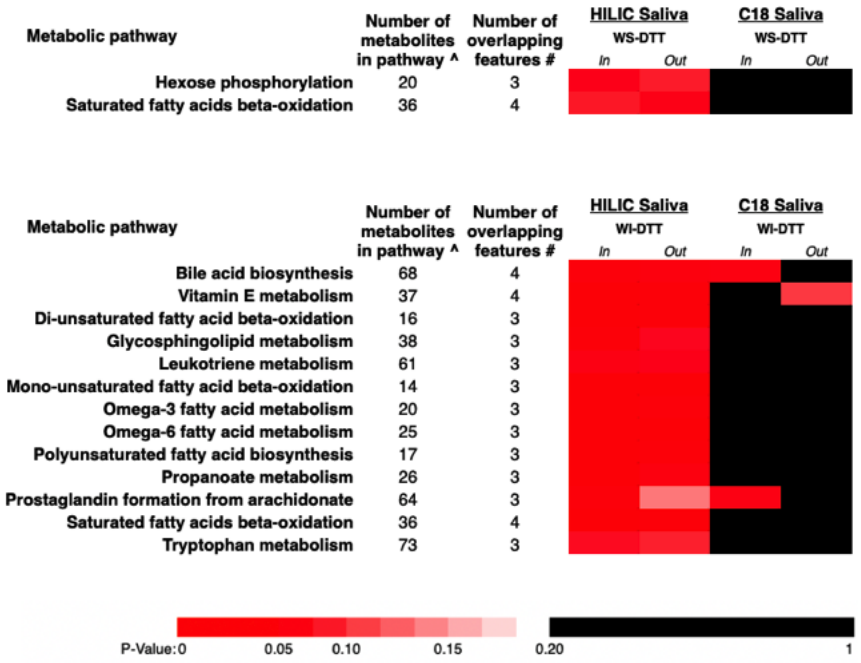

Figure 6. Metabolic pathways associated with ≥ 2 water soluable and insoluable FPMOP respectively in saliva.
Cells were shaded based on the p-value of the association between each of metabolic pathways and each indoor/ outdoor water soluble and insoluble FPMOP. Metabolic pathways are ordered according to the total number of the significant pathway-FPMOP associations ($p < 0.05$) in the HILIC column and the C18 column.
^ Total number of metabolites within the specific metabolic pathway;
# Number of significant metabolic features in the biosamples with m/z matched to the metabolites within the specific metabolic pathway.

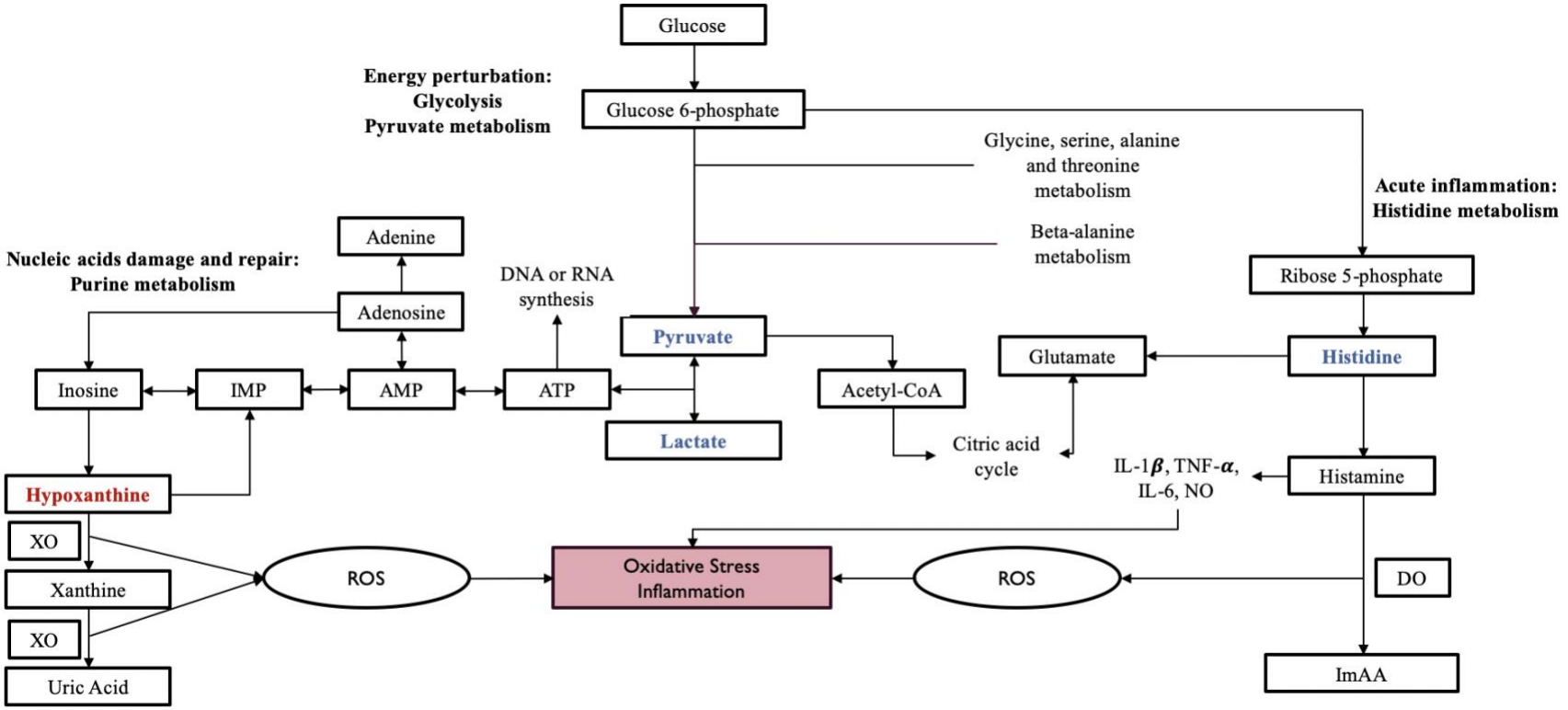

Figure 7. Potential molecular mechanisms underlying PM-related health impacts elucidated using untargeted high-resolution metabolomics on the study participants. Molecules in blue and red were confirmed metabolites in present analysis. Negative associations with increased FPMOP were denoted in blue and positive associations were denoted in red.
Acronym: ROS, reactive oxygen species; XO, xanthine oxidase; IMP, inosine monophosphate; AMP, adenosine monophosphate; ATP, adenosine triphosphate; DO, diamine oxidase; ImAA, imidazole acetic acid; IL-1 $\boldsymbol{\beta}$, the interleukin 1 $\boldsymbol{\beta}$; IL-6, the interleukin 6; TNF $\boldsymbol{\alpha}$, tumor necrosis factor alpha; NO, nitric oxide.

Table 1. Levels of FPMOP-related indicators and basic demographic characteristics of study participants.

Variable	Overall	Near Dorm	Far Dorm
Traffic pollutant levels (96h prior to biosamples collection)	-	-	-
$FPMOP^{WS\text{-}DTT}$ (nmol/min), mean (SD)	-	2.3 (1.0)	2.7 (1.0)
$FPMOP^{WI\text{-}DTT}$ (nmol/min), mean (SD)	-	3.7 (1.0)	3.8 (1.1)
$FPMOP^{total\text{-}DTT}$ (nmol/min), mean (SD)	-	6.0 (1.8)	6.6 (2.1)
$FPMOP^{WS\text{-}DTT}/m^3$ (nmol/min/m^3), mean (SD)	-	272.5 (81.2)	298.9 (88.4)
$FPMOP^{WS\text{-}DTT}$/μg (nmol/min/μg), mean (SD)	-	26.3 (8.3)	22.9 (3.9)
Demographic characteristics	N=54	N=24	N=30
Age (SD)	19.3 (0.8)	19.2 (0.9)	19.4 (0.8)
BMI(SD)	23.2 (3.2)	22.5 (3.2)	23.7 (3.1)
Days in Dorm prior to first plasma collection (SD)	69 (118)	87 (161)	54 (66)
Gender, n (%)	-	-	-
Female	25 (46)	12 (50)	13 (43)
Male	29 (54)	12 (50)	17 (57)
Academic year, n (%)	-	-	-
Freshmen	31 (57)	16 (67)	15(50)
Sophomore	15 (28)	3 (13)	12 (40)
Junior	7 (13)	4 (17)	3 (10)
Senior	1 (2)	1 (4)	0 (0)
Race, n (%)	-	-	-
African American	3 (6)	1 (4)	2 (7)
Asian	17 (31)	7 (29)	10 (33)
Mexican	1 (2)	0 (0)	1 (3)
White	33 (61)	16 (67)	17 (57)

Acronym: $FPMOP^{WS\text{-}DTT}$, oxidative potential of water-soluble fraction in fine particulate matter; $FPMOP^{WI\text{-}DTT}$, oxidative potential of water-insoluble fraction in fine particulate matter; $FPMOP^{total\text{-}DTT}$, oxidative potential of water-soluble fraction and water-insoluble fraction in fine particulate matter; $FPMOP^{WS\text{-}DTT}/m^3$, oxidative potential of water-soluble fraction in fine particulate matter normalized

by the total volume of sampled air; $FPMOP^{WS\text{-}DTT}/\mu g$, oxidative potential of water-soluble fraction in fine particulate matter divided by overall fine particulate mass; SD, standard deviation.

Table 2.
Mean indoor and outdoor levels of FPMOP-related metrics at near dorm and far dorm during the study period

Metrics	Indoor		Outdoor	
	Near Dorm	Far Dorm	Near Dorm	Far Dorm
$FPMOP^{WI\text{-}DTT}$	3.21 ± 0.70	3.62 ± 0.84	3.98 ± 1.09	3.64 ± 1.17
$FPMOP^{WS\text{-}DTT}$	1.84 ± 0.63	2.41 ± 0.77**	2.66 ± 0.82	2.86 ± 0.90
$FPMOP^{total\text{-}DTT}$	5.05 ± 1.20	6.03 ± 1.51*	6.51 ± 1.71	6.50 ± 1.94
$FPMOP^{WS\text{-}DTT}/m^3$	228.71 ± 53.72	277.98 ± 68.00**	301.09 ± 71.91	296.54 ± 85.85
$FPMOP^{WS\text{-}DTT}/\mu g$	36.07 ± 14.44	29.44 ± 11.31	29.06 ± 8.46	29.72 ± 12.35

Acronym: $FPMOP^{WI\text{-}DTT}$, oxidative potential of water-insoluble fraction in fine particulate matter; $FPMOP^{WS\text{-}DTT}$, oxidative potential of water-soluble fraction in fine particulate matter; $FPMOP^{total\text{-}DTT}$, oxidative potential of water-soluble fraction and water-insoluble fraction in fine particulate matter; $FPMOP^{WS\text{-}DTT}/m^3$, oxidative potential of water-soluble fraction in fine particulate matter normalized by the total volume of sampled air; $FPMOP^{WS\text{-}DTT}/\mu g$, oxidative potential of water-soluble fraction in fine particulate matter divided by overall fine particulate mass.

*p-value for Pooled t-Test or Mann-Whitney U Test < 0.05

** p-value for Pooled t-Test or Mann-Whitney U Test < 0.01

Table 3.

Number of significant metabolic features ($FDR_{B\text{-}H} < 0.2$) associated with FPMOP-related metrics in multiple biosample-technical columns.

Biosample-technical columns	Total number of extracted features	$FPMOP^{WI\text{-}DTT}$		$FPMOP^{WS\text{-}DTT}$		$FPMOP^{total\text{-}DTT}$		$FPMOP^{WS\text{-}DTT}/m^3$		$FPMOP^{WS\text{-}DTT}/\mu g$		Number of unique features[a]
		Indoor	Outdoor	Indoor	Outdoor	Indoor	Outdoor	Indoor	Outdoor	Indoor	Outdoor	
HILIC-plasma	13,419	207	121	292	220	229	132	214	110	145	204	967
C18-plasma	7,347	97	80	156	149	118	59	120	53	71	94	545
HILIC-saliva	21,313	230	199	299	206	278	189	264	187	212	168	1,214
C18-saliva	7,700	70	74	84	77	78	75	79	70	90	76	412

Acronym: $FPMOP^{WI\text{-}DTT}$, oxidative potential of water-insoluble fraction in fine particulate matter; $FPMOP^{WS\text{-}DTT}$, oxidative potential of water-soluble fraction in fine particulate matter; $FPMOP^{total\text{-}DTT}$, oxidative potential of water-soluble fraction and water-insoluble fraction in fine particulate matter; $FPMOP^{WS\text{-}DTT}/m^3$, oxidative potential of water-soluble fraction in fine particulate matter normalized by the total volume of sampled air; $FPMOP^{WS\text{-}DTT}/\mu g$, oxidative potential of water-soluble fraction in fine particulate matter divided by overall fine particulate mass; $FDR_{B\text{-}H}$, Benjamini-Horchberg false discover rate procedure.

[a] Number of unique metabolic features that are significantly ($FDR_{B\text{-}H} < 0.2$) associated with ≥ 1 FPMOP-related metrics.

Table 4.

Chemical identity[a] of the metabolic features significantly associated with FPMOP-related indicators ($FDR_{B\text{-}H} < 0.2$) in the DRIVE study.

m/z	RT (s)	Validated metabolite	Adduct form	Associated FPMOP-related indicators	Biometric column
137.0463	44.2	Hypoxanthine	M+H	Indoor: $FPMOP^{WS\text{-}DTT}$/μg (β = 0.094)	HILIC-plasma
156.0773	101.0	Histidine	M+H	Outdoor: $FPMOP^{WS\text{-}DTT}$/μg (β = -0.050)	HILIC-saliva
87.0083	19.8	Pyruvate	M-H	Indoor: $FPMOP^{total\text{-}DTT}$ (β = -0.180) $FPMOP^{WS\text{-}DTT}/m^3$ (β = -0.004) $FPMOP^{WI\text{-}DTT}$ (β = -0.235) $FPMOP^{WS\text{-}DTT}$ (β = -0.271)	C18-plasma
89.0239	22.2 22.9	Lactate, glyceraldehyde	M-H	Indoor: $FPMOP^{total\text{-}DTT}$ (β = -0.269) $FPMOP^{WS\text{-}DTT}/m^3$ (β = -0.006) $FPMOP^{WI\text{-}DTT}$ (β = -0.321) $FPMOP^{WS\text{-}DTT}$ (β = -0.450)	C18-plasma
154.0617	23.0	Histidine	M-H	Indoor: $FPMOP^{WS\text{-}DTT}$ (β = -0.378)	C18-plasma
187.0971	25.2	Azelaic acid	M-H	Indoor: $FPMOP^{WS\text{-}DTT}$/μg (β = -0.020) $FPMOP^{WS\text{-}DTT}/m^3$ (β = -0.002) $FPMOP^{WI\text{-}DTT}$ (β = -0.181)	C18-plasma
281.2481	257.4 256.8 258.0	Petroselinic acid, Elaidic acid, Oleate	M-H	Indoor: $FPMOP^{total\text{-}DTT}$ (β = -0.721)	C18-plasma

Acronym: m/z, mass to charge ratio; RT, retention time; $FPMOP^{WS\text{-}DTT}$/μg, oxidative potential of water-soluble fraction in fine particulate matter divided by overall fine particulate mass; $FPMOP^{WS\text{-}DTT}/m^3$, oxidative potential of water-soluble fraction in fine particulate matter normalized by the total volume of sampled air; $FPMOP^{WS\text{-}DTT}$, oxidative potential of water-soluble fraction in fine

particulate matter; $FPMOP^{WI\text{-}DTT}$, oxidative potential of water-insoluble fraction in fine particulate matter; $FPMOP^{total\text{-}DTT}$, oxidative potential of water-soluble fraction and water-insoluble fraction in fine particulate matter.

[a] Chemical confirmation on the candidate metabolic features was conducted by matching peaks by accurate mass and retention time to authentic reference standards in an in-house library run under identical conditions using tandem mass spectrometry.

Supplementary Tables and Figures.

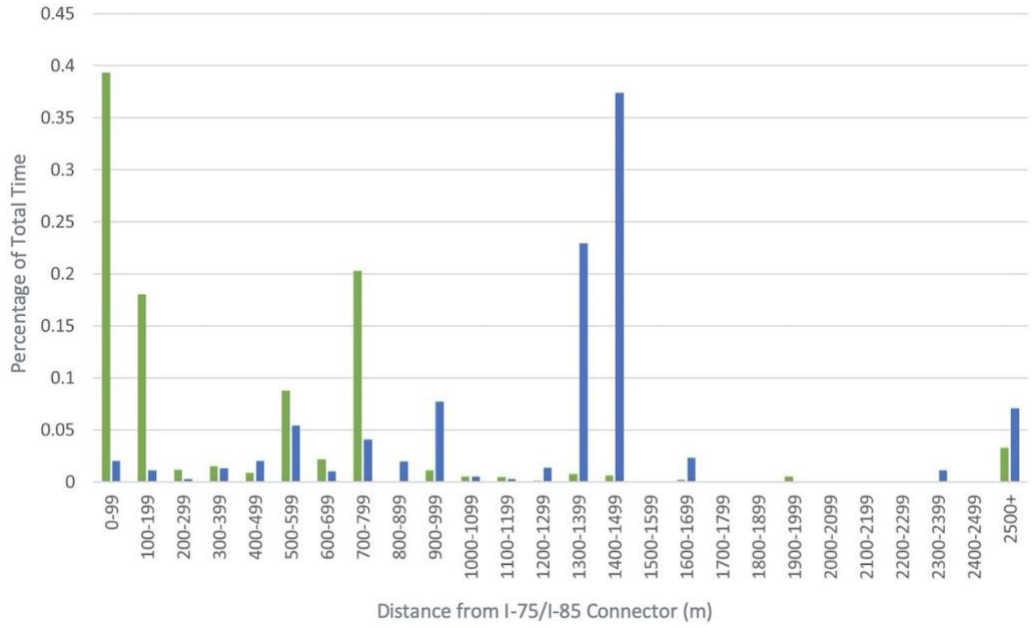

Figure S1. Percentage of total time spent by participants by linear distance to the I-75/I-85 Connector. Green bars represent distribution of time among students living in the Near Dorm and blue bars represent distribution of time among students living in the Far Dorm.

Table S1.

Geometric mean of FPMOP-related indicators (96h prior to biosamples collection) of study participants.

FPMOP-related indicators, geometric mean (SD)	**Near Dorm**	**Far Dorm**
$FPMOP^{WS\text{-}DTT}$ (nmol/min)	2.1 (1.5)	2.6 (1.4)
$FPMOP^{WI\text{-}DTT}$ (nmol/min)	3.5 (1.3)	3.7 (1.4)
$FPMOP^{total\text{-}DTT}$ (nmol/min)	5.7 (1.4)	6.3 (1.3)
$FPMOP^{WS\text{-}DTT}/m^3$ (nmol/min/m^3)	261.6 (1.3)	288.0 (1.3)
$FPMOP^{WS\text{-}DTT}$/μg (nmol/min/μg)	25.1 (1.3)	22.6 (1.2)

Acronym: $FPMOP^{WS\text{-}DTT}$, oxidative potential of water-soluble fraction in fine particulate matter; $FPMOP^{WI\text{-}DTT}$, oxidative potential of water-insoluble fraction in fine particulate matter; $FPMOP^{total\text{-}DTT}$, oxidative potential of water-soluble fraction and water-insoluble fraction in fine particulate matter; $FPMOP^{WS\text{-}DTT}/m^3$, oxidative potential of water-soluble fraction in fine particulate matter normalized by the total volume of sampled air; $FPMOP^{WS\text{-}DTT}$/μg, oxidative potential of water-soluble fraction in fine particulate matter divided by overall fine particulate mass; SD, standard deviation.

Table S2.

Number of significant metabolic features ($FDR_{B\text{-}H} < 0.05$) associated with FPMOP-related metrics in multiple biosample-technical columns.

Biosample-technical columns	Total number of extracted features	$FPMOP^{WI\text{-}DTT}$		$FPMOP^{WS\text{-}DTT}$		$FPMOP^{total\text{-}DTT}$		$FPMOP^{WS\text{-}DTT}/m^3$		$FPMOP^{WS\text{-}DTT}/\mu g$		Number of unique features[a]
		Indoor	Outdoor	Indoor	Outdoor	Indoor	Outdoor	Indoor	Outdoor	Indoor	Outdoor	
HILIC-plasma	13,419	83	89	131	109	115	93	104	82	104	113	498
C18-plasma	7,347	57	51	82	78	61	47	68	41	49	49	307
HILIC-saliva	21,313	147	138	185	137	198	120	188	121	145	114	783
C18-saliva	7,700	50	49	57	43	65	46	67	47	63	48	264

Acronym: $FPMOP^{WI\text{-}DTT}$, oxidative potential of water-insoluble fraction in fine particulate matter; $FPMOP^{WS\text{-}DTT}$, oxidative potential of water-soluble fraction in fine particulate matter; $FPMOP^{total\text{-}DTT}$, oxidative potential of water-soluble fraction and water-insoluble fraction in fine particulate matter; $FPMOP^{WS\text{-}DTT}/m^3$, oxidative potential of water-soluble fraction in fine particulate matter normalized by the total volume of sampled air; $FPMOP^{WS\text{-}DTT}/\mu g$, oxidative potential of water-soluble fraction in fine particulate matter divided by overall fine particulate mass; $FDR_{B\text{-}H,}$ Benjamini-Horchberg false discover rate procedure.

[a] Number of unique metabolic features that are significantly ($FDR_{B\text{-}H} < 0.05$) associated with ≥ 1 FPMOP-related metrics.